Particle profiling of EV-lipoprotein mixtures by AFM nanomechanical imaging

Supporting Information

Preparation of RBC-EVs

Blood samples were obtained by healthy donors from Spedali Civili hospital (Brescia, Italy) with informed consents. All experiments with human blood samples were performed according to the guidelines and the approval of the Spedali Civili Ethics committee.

RBC-EVs were isolated following the protocol from Usman et al [Usman 2018, Nyugen 2016]. Briefly, after blood collection, RBCs were pelleted by centrifugation at 1000 × *g* for 8 minutes at 4°C (5804R Eppendorf centrifuge, A-4-44 rotor, 15 ml tubes) and washed three times in PBS (Corning, USA). RBCs were further washed two times with CPBS [PBS + 0.1 g/L calcium chloride (Sigma Aldrich, St. Louis, USA)] and transferred into a 75 mm^2 tissue culture flask (Corning, USA). Calcium ionophore (A23187, Sigma Aldrich, St. Louis, USA) was added to the flask (final concentration 10 mM) and incubated overnight at 37°C.

To separate EVs, RBCs and cell debris were removed by differential centrifugation (600 × *g* for 20 min, 1600 × *g* for 15 min, 3260 × *g* for 15 min, and 10,000 × *g* for 30 min at 4 °C). The pellet was discarded at every step, transferring the supernatant to a fresh tube. The supernatants were filtered through 0.45 µm nylon syringe filters (Sarstedt, Germany).

EVs were concentrated by ultracentrifugation at 100,000 × g for 70 min at 4 °C (Optima XPN-100, TY45 Ti rotor, Beckman Coulter, USA). EV pellets were then resuspended in cold PBS, layered above 2 ml frozen 60% sucrose cushion and centrifuged at 100,000 × *g* for 16 h at 4 °C (Optima MAX-XP, MLS-50 rotor, Beckman Coulter, USA), with deceleration speed set to 0. The red layer of EVs was collected and washed twice with cold PBS and spun at 100,000 × *g* for 70 min at 4 °C (Optima MAX-XP, TLA-55 rotor, Beckman Coulter). Finally, EVs were resuspended in 1 ml of cold PBS.

[Nguyen 2016]: Nguyen, D. B., Thuy Ly, T. B., Wesseling, M. C., Hittinger, M., Torge, A., Devitt, A., Perrie, Y., & Bernhardt, I. (2016). Characterization of Microvesicles Released from Human Red Blood Cells. Cellular Physiology and Biochemistry : International Journal of Experimental Cellular Physiology, Biochemistry, and Pharmacology, 38(3), 1085–1099. https://doi.org/10.1159/000443059

[Usman 2018]: Usman, W. M., Pham, T. C., Kwok, Y. Y., Vu, L. T., Ma, V., Peng, B., Chan, Y. S., Wei, L., Chin, S. M., Azad, A., He, A. B. L., Leung, A. Y. H., Yang, M., Shyh-Chang, N., Cho, W. C., Shi, J., & Le, M. T. N. (2018). Efficient RNA drug delivery using red blood cell extracellular vesicles. Nature Communications 2018 9:1, 9(1), 1–15. https://doi.org/10.1038/s41467-018-04791-8

Preparation of hCPC-EVs

EVs were isolated from media conditioned (CM) by CPC . Briefly, CPCs (70-80 % confluent) were washed twice with DPBS and incubated at 37°C with 5% CO_2 in DMEM 4.5 g/l glucose without phenol red (Gibco/Thermo Fisher Scientific). After 7 days, the CM was clarified by 0.22 μm filtration through bottle filter units or on-line filters (ULTA Capsule HC, KMP-HC9202HH, GE Healthcare, USA). Concentration and EV size selection were performed by tangential flow filtration (TFF), using the ÄKTA™ flux 6 system (GE Healthcare) equipped with a 300 kDa cut-off hollow fiber cartridge (GE Healthcare); the concentration was followed by diafiltration in 5 volumes of Plasma-Lyte A® solution.

[Andriolo 2018]: Andriolo, G., Provasi, E., lo Cicero, V., Brambilla, A., Soncin, S., Torre, T., Milano, G., Biemmi, V., Vassalli, G., Turchetto, L., Barile, L., & Radrizzani, M. (2018). Exosomes from human cardiac progenitor cells for therapeutic applications: Development of a GMP-grade manufacturing method. *Frontiers in Physiology*, *9*(AUG), 1169. https://doi.org/10.3389/FPHYS.2018.01169

Table S1

Sample	*Particle/mL (NTA)*	*Diameter (NTA)*	*Diameter (DLS)*	*D_{eq} (AFM)*	*Diameter (cryoEM)*
HDLs	NA	NA	10 ± 1 nm	10 ± 5 nm	12 ± 4 nm
IDLs	NA	NA	17 ± 3 nm	17 ± 2 nm	20 ± 3 nm
LDLs	NA	NA	47 ± 3 nm	19 ± 3 nm	23 ± 13 nm
VLDLs	$2.5*10^{12} \pm 1.2*10^{7}$	148 ± 3 nm	128 ± 2 nm	27 ± 10 nm	43 ± 32 nm
Chylomicrons	$3.3*10^{12} \pm 2.3*10^{7}$	178 ± 4 nm	174 ± 5 nm	60 ± 50 nm	80 ± 59 nm
hCPC-EVs	$1.0*10^{11} \pm 4.3*10^{6}$	193 ± 2 nm	62 ± 1 nm	42 ± 11 nm	NA
RBC-EVs	$1.81*10^{12} \pm 8.8*10^{10}$	160 ± 2.3 nm	180 ± 4 nm	112 ± 36 nm	NA

Table S1 *– particle concentration and hydrodynamic diameter by NTA; hydrodynamic diameter by DLS; geometric diameter by AFM and cryoEM. Reported variances are the standard deviations of the averages over multiple experiments for NTA (N=3) and DLS (N=10); AFM and cryoEM variances are instead the standard deviations of all measured particles (N between 135 and 510) over multiple depositions/experiments, and should be purely viewed as a rough indicator of polydispersity, since several of the size distributions were found to be multimodal (see main text Figure 2). Some of the entries are labeled as not available (NA), for different reasons: NTA was not able to detect any particle in the HDL, LDL and IDL samples, and too few intact EVs were observed via cryoEM to give a significant estimate. It is interesting to note that while AFM and cryoEM largely agree on the size of all particles, NTA and DLS measurements deviate from those values, although in a reproducible manner as evidenced by the low variances. Despite these limitations, we chose to include NTA and DLS readings of all samples as examples of typical readouts given by those techniques.*

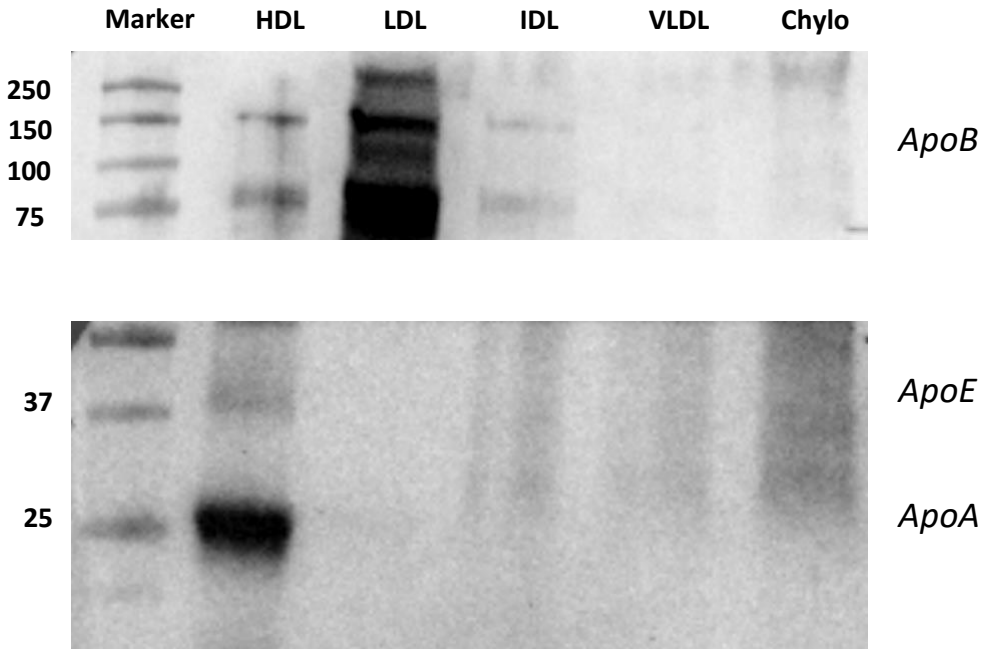

Figure S1 *– Western Blotting analysis for all lipoproteins sub-classes confirms the presence of typical Apolipoprotein signals. As expected, ApoA is prevalent in HDLs while ApoB is extremely abundant in LDLs but also present in other sub-classes.*

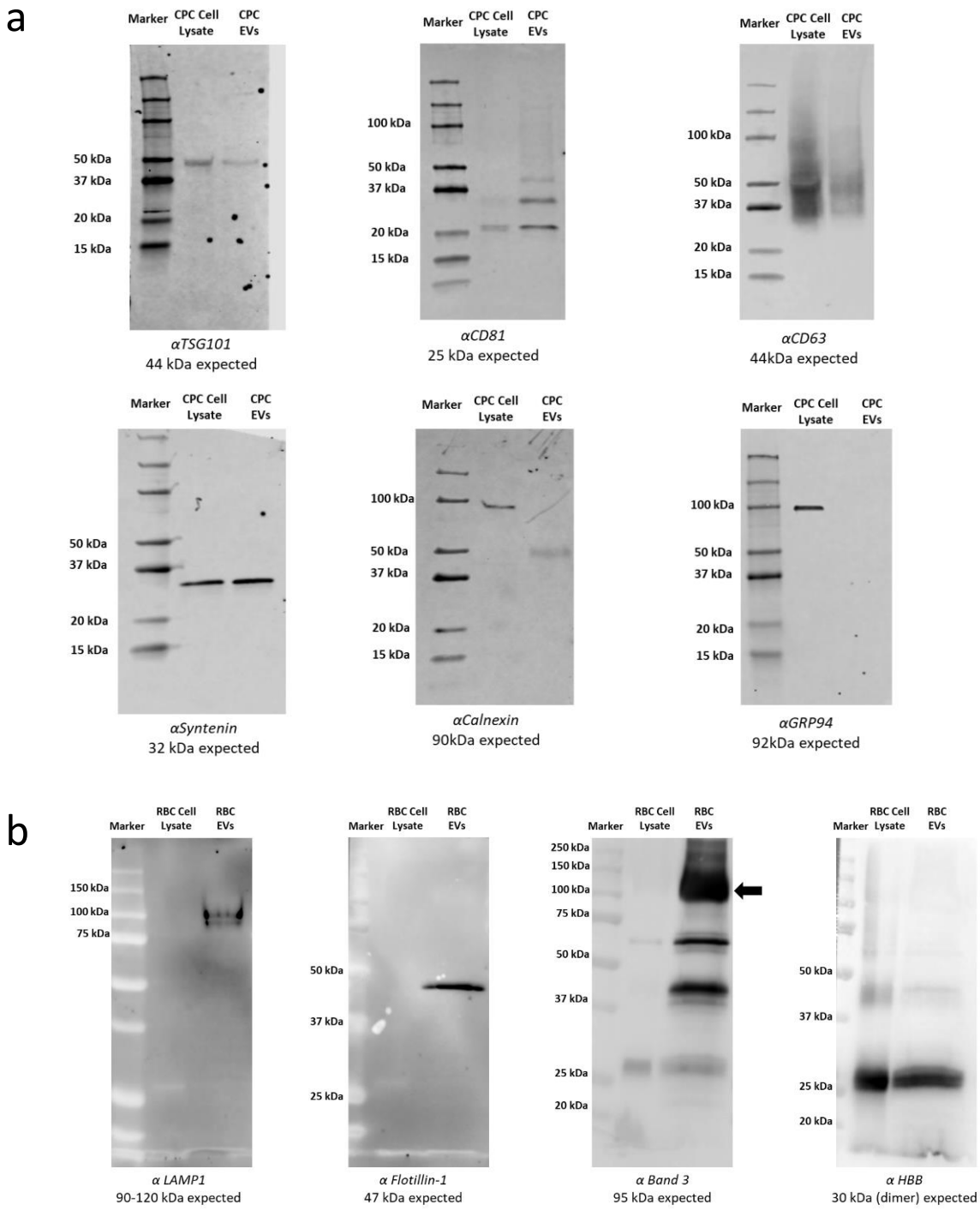

Figure S2 *– (a): Western Blotting analysis for the hCPC-EVs samples confirms the presence of luminal proteins TSG101 and Alix and of transmembrane tetraspanins CD81 and CD63. As expected, GRP94 and Calnexin are instead only present in the cell lysates. (b): Western Blotting analysis of the RBC-EVs samples confirms the presence of transmembrane, membrane-associated, and luminal proteins. Specifically, RBC-EV samples were enriched in LAMP-1 and Flotillin-1 as membrane-associated proteins, Band 3 as a transmembrane protein, and Hemoglobin-β (HBB) as a luminal protein. Band 3 and HBB are considered as markers of both RBCs and RBC-derived EVs (https://doi.org/10.3389/fmed.2021.761362). 20µg proteins of RBC lysates and RBC-EVs samples were loaded, and signals were detected after 10 seconds (BAND-3 and HBB), 12 minutes (LAMP1), and 9 minutes (Flotillin-1).*

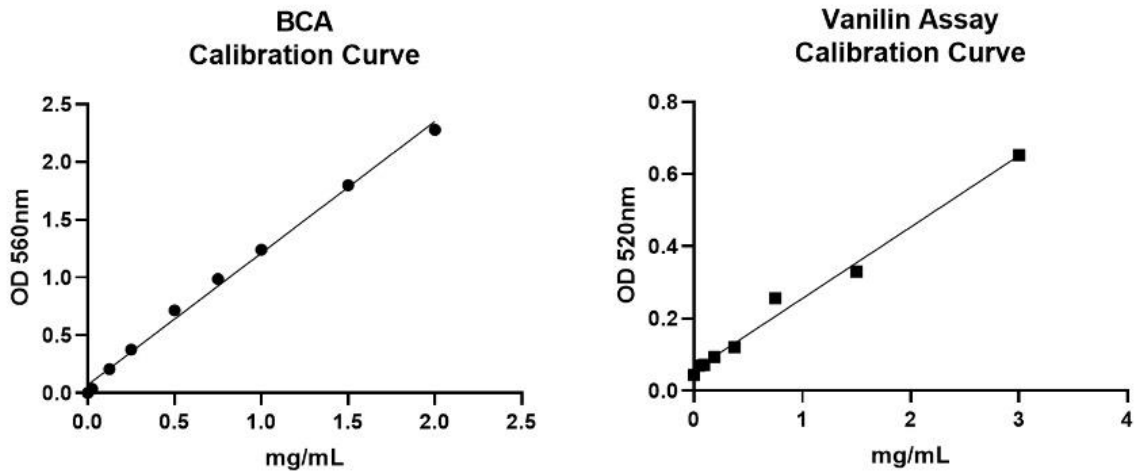

Sample	BCA (mg/mL)	Lipids (mg/mL)	Ratio
HDL	402,21	285,69	1,41
LDL	347,64	462,01	0,75
IDL	0,47	2,61	0,18
VLDL	0,45	1,75	0,26
Chilo	1,37	15,30	0,09
EVs	2,10	1,49	1,40

Figure S3 *– BCA and Lipid concentration assay for Lipoproteins and hCPC EVs. Upper panels: calibration curves run with Bovine Serum Albumin (BSA) for the BCA test on the left and DOPC standards for* sulfo-phopsho-vanillin *test on the right. Accordingly, table reports protein content, lipid content and protein/lipid ratio for each analyzed sample.*

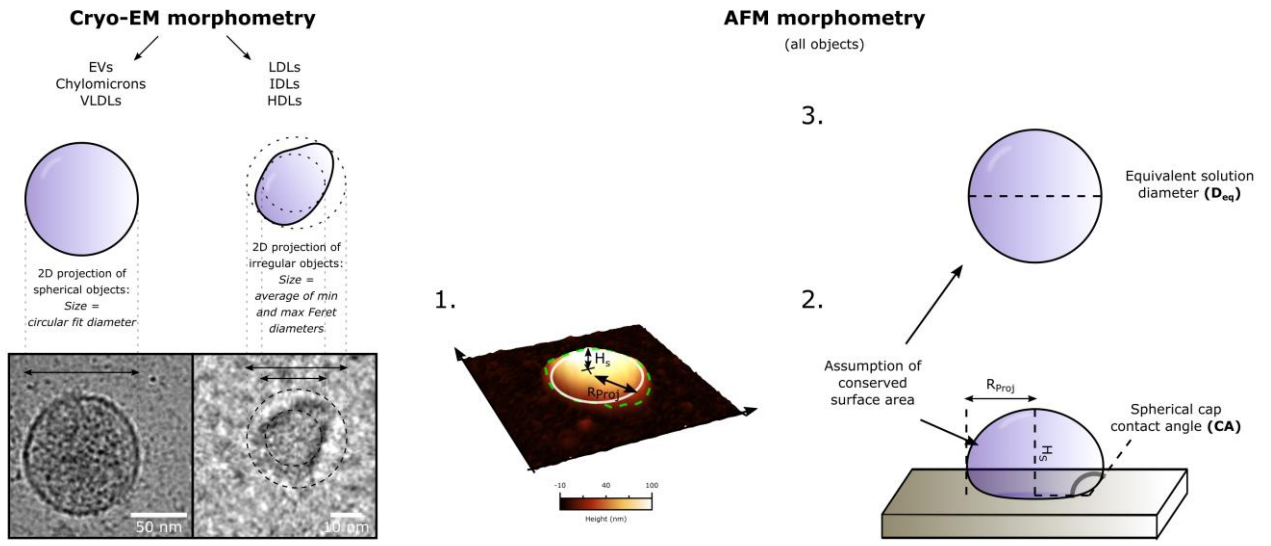

Figure S4 *– (Left): Quantitative Cryo-EM morphometry procedure for spherical (EVs, Chylomicrons, VLDLs) and irregular (LDLs, IDLS, HDLs) objects. Spherical objects: direct circular fit. Irregular objects: average of maximum and minimum Feret diameters (see materials and methods). The resulting size distributions are shown in main text figure 2.*

(Right): Measurement of the equivalent solution diameter (D_{eq}) and equivalent spherical cap contact angle (CA) of an unknown particle via AFM morphometry. (1): The height (H_s) and maximum inscribed disc radius (R_{proj}) of discrete objects are measured on AFM micrographs. (2): The object's geometry is approximated with a spherical cap of height H_s and projected radius $R_{proj.}$ It is then possible to calculate its surface contact angle (CA). Please refer to main text reference [Ridolfi 2020a] for additional details on the procedure. (3): The diameter of a sphere having the same surface area of the spherical cap introduced at step 2 is calculated. The resulting 'equivalent solution siameter' (D_{eq}) size distributions are shown in figure 2. It is unnecessary to know whether the analysed particle is an EV or a LP. However, if the particle's nanomechanics are those of an intact vesicle, the CA recapitulates its mechanical stiffness (see main text); if the particle's nanomechanical behaviour is not known (as for LPs), CA is just a robust numerical descriptor of their geometry. CA values from hundreds of individual objects were pooled in the CA/Deq plots shown in main text figure 3.

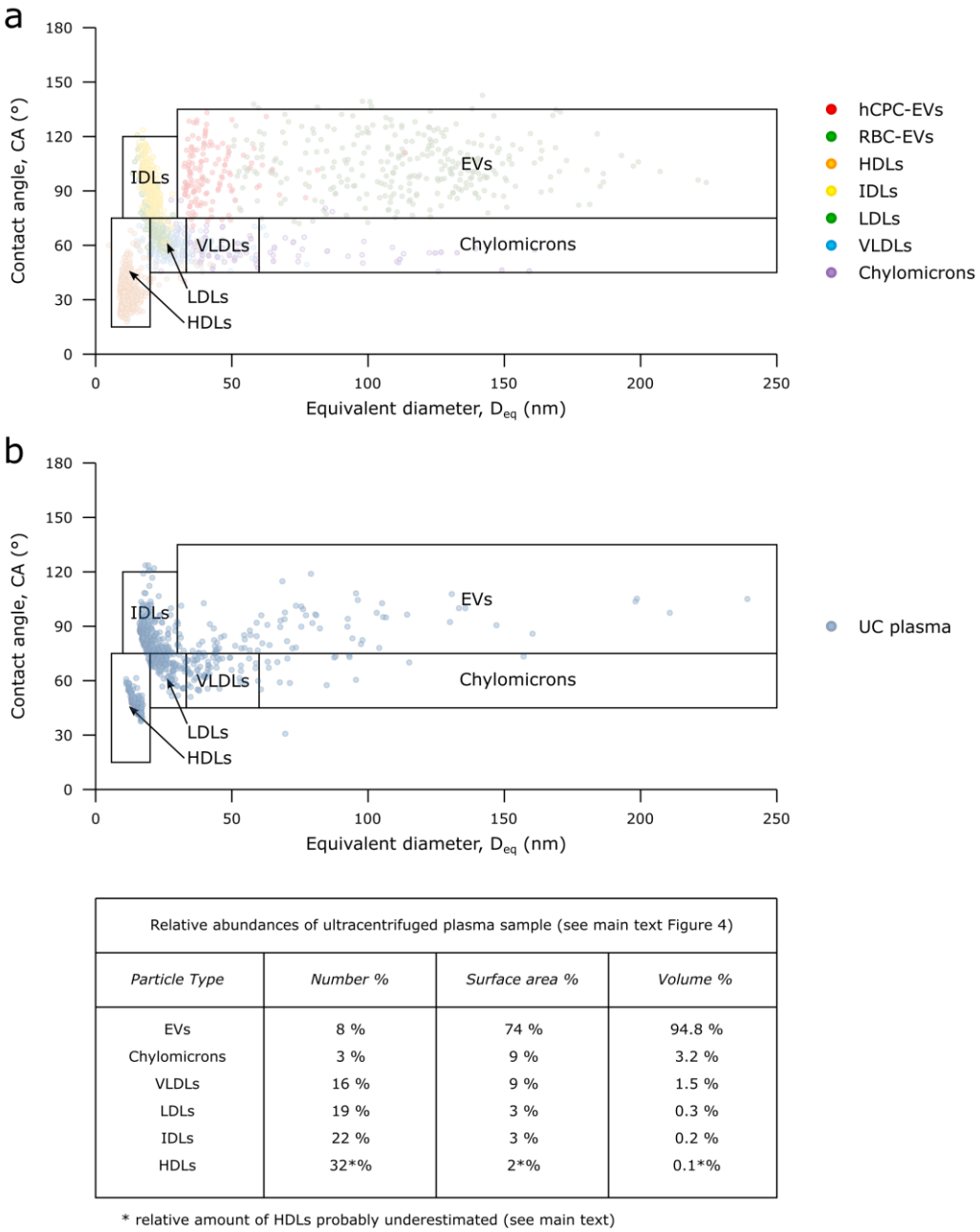

Relative abundances of ultracentrifuged plasma sample (see main text Figure 4)			
Particle Type	*Number %*	*Surface area %*	*Volume %*
EVs	8 %	74 %	94.8 %
Chylomicrons	3 %	9 %	3.2 %
VLDLs	16 %	9 %	1.5 %
LDLs	19 %	3 %	0.3 %
IDLs	22 %	3 %	0.2 %
HDLs	32*%	2*%	0.1*%

* relative amount of HDLs probably underestimated (see main text)

Figure S5 *– (a): assignment of biological identity to discrete zones of a CA/D_{eq} scatterplot. (b): Relative abundances of particles corresponding to each identity in the ultracentrifuged plasma sample (see main text Figure 3c) as estimated via the assignments shown in panel (a). Abundances are given in terms of: percentage of particles in that class with respect to total number of particles (left column), percentage of surface area exposed by particles in that class with respect to total exposed surface area (middle column), and percentage of volume enclosed by particles in that class with respect to total volume of all particles. Surface areas and volumes of individual particles can be calculated by trivial trigonometry using the same morphological parameters (H_s and R_{proj}) described in Figure S4.*

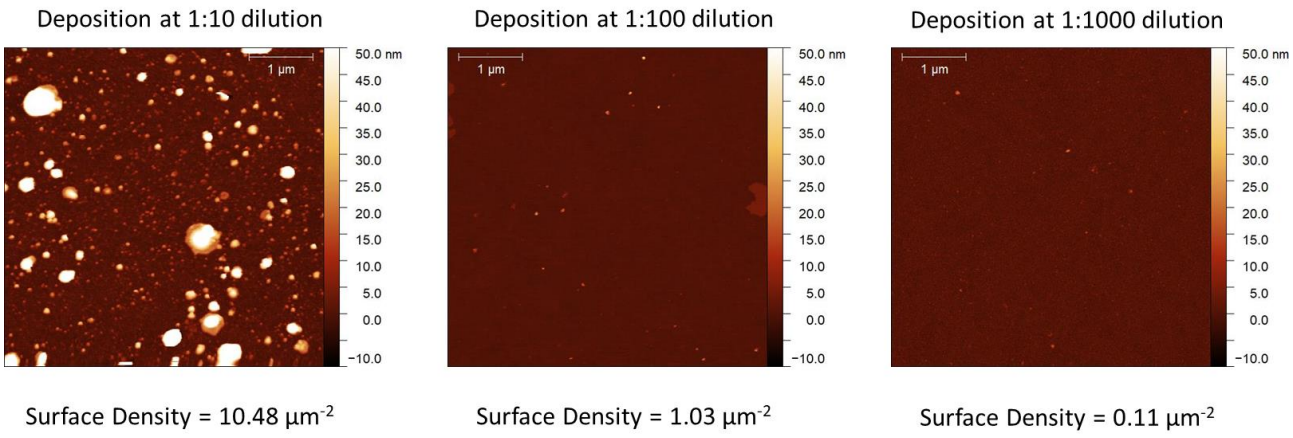

Figure S6 *– Linear correlation between sample deposition concentration and the resulting surface density of deposited particles. The same ultracentrifuged plasma sample of Figures 3c and S5 was deposited as described in the main text (see materials and methods) at increasing 10x dilutions. The sample is highly heterogeneous and comprises both EVs and LPs, but the total surface density of all particles remains linearly correlated to deposition dilution across two orders of magnitude (R^2=0.99). This suggests that, following the deposition protocol described in the main text, and taking care that the surface is not fully saturated, all classes of particles are able to fully adsorb on the substrate, with no apparent quantitative biases due to different kinetics or substrate affinities.*